ChemPubSoc Europe

DOI: 10.1002/chem.201404292

CHEMISTRY
A European Journal
Full Paper

Bioimaging

BODIPY-Based Oligo(ethylene glycol) Dendrons as Fluorescence Thermometers: When Thermoresponsiveness Meets Intramolecular Electron/Charge Transfer**

Hua Wang,[a] Yongquan Wu,[b] Pan Tao,[c] Xing Fan,[c] and Gui-Chao Kuang*[a]

Abstract: The temperature-dependent photophysical properties of a series of 4,4-difluoro-4-bora-3a,4a-diaza-s-indacene (BODIPY) derivatives with different oligo(ethylene glycol) (OEG) dendrons were investigated. Weak fluorescence emission was observed for these BODIPY derivatives in dilute solution with low viscosity. BDP-G0 and BDP-G1-TEG exhibit a high quantum yield in viscous glycerol solutions, contrary to the moderate and little fluorescence enhancement for BDP-G1 and BDP-G2 under the same conditions. The photoinduced electron transfer (PET) may have quenched the fluorescence, as supported by calculation. Interestingly, the thermoresponsive BODIPY derivatives show heat-induced luminescence enhancement with a high signal-to-noise ratio and their emission maxima are dependent on the structures of branched tri(ethylene glycol) moieties. Finally, preliminary studies on the BODIPY derivatives as intracellular fluorescence indicators in living HeLa cells were carried out.

Introduction

Molecular fluorescence thermometers with a long wavelength emission and biocompatible properties are powerful tools as sensors in biological imaging application.[1] Among various fluorescence thermometers, the compounds showing strong fluorescence intensities are good candidates due to their high signal-to-noise ratio. The most well-reported molecular fluorescence thermometers are based on viscosity or polarity sensitive dyes, whose quenching pathway is impaired during the thermo-dehydration process, which restores their fluorescence emission.[2] Various kinds of polymeric fluorescence thermometers have been applied in intracellular temperature measurement.[3] However, to realize their widespread biological application and to overcome several drawbacks such as illumination brightness, excitation source fluctuations, and photobleaching,[4] researchers turn their attention to investigate the fluorescence properties of thermoresponsive dendrimers due to their advantages derived from a uniform structure and a tunable functionality.[5] Although a few works referring to luminescent dendrimers, which display thermoresponsive properties, have been demonstrated,[6] the emission intensities of these thermometers decrease in the heating process, which is not desired as fluorescence turn-on type of sensors. Therefore, it is challenging to develop thermoresponsive dendrimers, which show heat-induced fluorescence intensities.

4,4-Difluoro-4-bora-3a,4a-diaza-s-indacene (BODIPY, which is abbreviated as BDP in the text) dyes bare excellent features such as high extinction coefficients, a long wavelength emission ($\geq$500 nm), high fluorescence quantum yields, and narrow emission bandwidths.[7] BDP derivatives therefore have been adopted in fluorescence sensors and biotechnology. In fact, a BDP core with a phenyl substituent at the *meso* position has been extensively investigated. The spectroscopic properties could be tuned by the substituents on the BDP cores and on the benzene moieties.[8] On one hand, the fluorescence intensity would be restored for the *meso*-phenyl BDP derivative without *ortho* substituents in viscous solutions, which usually slow down intramolecular rotation.[9] These BDP derivatives were utilized to measure the microviscosity in live cells by determining their fluorescence life time values.[10] On the other hand, the fluorescence properties are dependent on the solvents polarity, a twisted intramolecular charge-transfer (TICT) process at polar solvents would be involved for the BDP derivatives containing donor and acceptor units.[11]

Thermoresponsive BDP derivatives will not only show a special photophysical behavior but also provide a convenient way to alter their fluorescence properties.[2c,12] It is of our interest to develop a thermoresponsive polymer bearing BDP fluorophores to gain a molecular insight into the thermo-reversible phase separation.[13] Though several water-soluble amphiphilic BDP dyes with thermoresponsive branched tri(ethylene glycol) moieties have been reported, attentions have focused on their

[a] *H. Wang, Prof. Dr. G.-C. Kuang*
Department of Polymer Materials, Shanghai University
Nanchen Road 333, 200444, Shanghai (P.R. China)
E-mail: gckuang@shu.edu.cn

[b] *Dr. Y. Wu*
Department of Chemistry, Fudan University
Handan Road 220, 200433, Shanghai (P.R. China)

[c] *P. Tao, Prof. Dr. X. Fan*
College of Chemistry and Chemical Engineering, Chongqing University
Shazheng Road 174, 400044, Chongqing (P.R. China)

[**] *BODIPY = 4,4-difluoro-4-bora-3a,4a-diaza-s-indacene.*

Supporting information for this article is available on the WWW under http://dx.doi.org/10.1002/chem.201404292.

photodynamic therapy[14] and photophysical properties,[15] The thermoresponsive properties of this class of compounds and their applications in live cell imaging have not been reported.

Our group is interested in the synthesis of oligo(ethylene glycol) (OEG) dendrimers/dendronized polymers and the investigation of their thermoresponsive properties.[13,16] In this work, a series of amphiphilic BDP derivatives (Scheme 1) were prepared and their thermoresponsive and photophysical properties were studied. The mechanisms responsible for the fluorescence enhancement in aqueous solution during the heating process were examined. In addition, the potential of the BDP derivatives as intracellular fluorescent indicators for bioimaging in HeLa cells was evaluated by laser scanning fluorescence microscopy (LSFM).

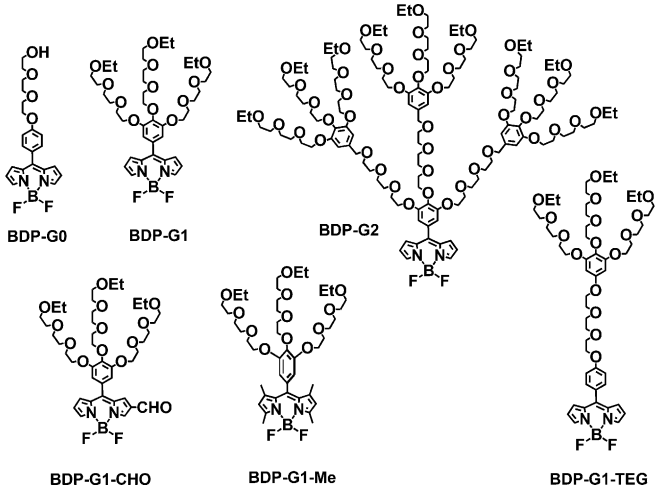

Scheme 1. Structures of the BDP derivatives studied in the present work.

Results and Discussion

Design and Synthesis of the BDP derivatives

BDP-G*n* ($n=0$, 1, and 2), BDP-G1-TEG, and BDP-G1-Me were prepared similarly. These BDP derivatives were synthesized by following well-reported procedures (Scheme 2).[7] Formyl-modified OEG dendrons followed a classic synthetic pathway, that is acid-catalyzed condensation with pyrrole, then oxidation with *p*-chloranil, and finally complexation with boron trifluoride etherate, to afford the target BDP derivatives. Three model compounds BDP-G1-Me, BDP-G1-CHO, and BDP-G1-TEG were prepared as well. These new compounds were characterized by NMR spectroscopy and high-resolution mass spectrometry (see the Supporting Information).

Spectroscopic properties of the BDP derivatives in dilute solution

The absorption and emission spectra of the BDP derivatives in various solvents were collected (Figure 1). The spectral profiles are almost identical and show less than 8 nm shift in various solvents (except for BDP-G2 in glycerol and BDP-G1-CHO), indicating no significant donor–acceptor interaction in the ground state. The absorption and emission peak values and the relative φ_{fl} values are summarized in the Table 1. These BDP derivatives could be divided to three types depending on the φ_{fl} values: 1) BDP-G0 and BDP-G1-TEG with one-folded OEG substituent on the phenyl ring (close to the BDP fluorophore) are considered as the first type, both show a weak emission in low

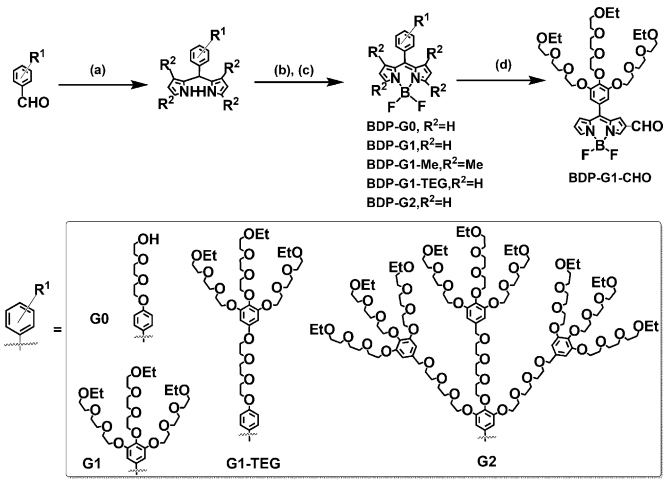

Scheme 2. Synthetic procedure for the BDP derivatives. a) trifluoroacetic acid (TFA), pyrrole, RT, 18 h. b) *p*-Chloranil, dichloromethane, −5 °C–RT. c) TEA, BF_3·OEt_2, RT. d) $POCl_3$, DMF, 1,2-dichloethane, K_2CO_3, 0–60 °C, 6 h (78 %).

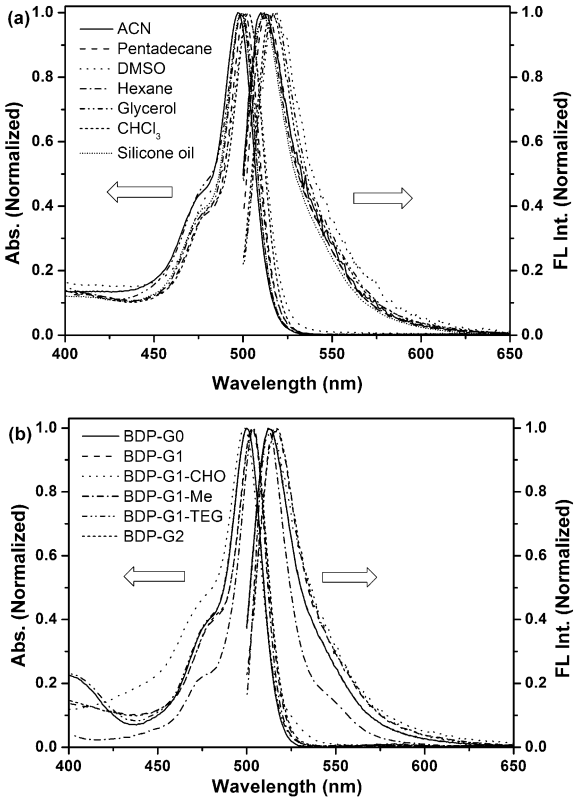

Figure 1. Normalized absorption and emission spectra of a) BDP-G1 (2.0 μM) in various solvents and b) the BDP derivatives (2.0 μM) in chloroform. $\lambda_{ex}=490$ nm.

Table 1. Spectroscopic data for the BDP derivatives.[a]

Comp.	Solvent[b]	λ_{abs} [nm]	λ_{em} [nm]	φ_{fl}	Comp.	Solvent	λ_{abs} [nm]	λ_{em} [nm]	φ_{fl}
BDP-G0	HEX	498	509	0.026	BDP-G1-TEG	HEX	497	509	0.019
	PEN	500	512	0.036		PEN	499	511	0.030
	SIO[c]	497	510	0.032		SIO[c]	498	510	0.036
	$CHCl_3$	500	512	0.040		$CHCl_3$	500	514	0.039
	GLY[d]	495	512	0.466		GLY[d]	497	513	0.196
	ACN	494	510	0.013		ACN	495	509	0.013
	DMSO	500	515	0.019		DMSO	500	516	0.018
BDP-G1	HEX	499	512	0.014	BDP-G1-Me	HEX	501	508	0.392
	PEN	501	513	0.023		PEN	502	510	0.363
	SIO[c]	500	511	0.023		SIO[c]	500	508	0.381
	$CHCl_3$	503	517	0.013		$CHCl_3$	504	512	0.408
	GLY[d]	499	518	0.033		GLY[d]	501	510	0.322
	ACN	497	510	0.001		ACN	498	506	0.109
	DMSO	503	519	0.002		DMSO	502	511	0.082
BDP-G2	HEX	501	511	0.008	BDP-G1-CHO	HEX	497	509	0.007
	PEN	507	516	0.002		PEN	499	511	0.012
	SIO[c]	501	515	0.013		SIO[c]	496	509	0.008
	$CHCl_3$	503	517	0.014		$CHCl_3$	499	515	0.003
	GLY[d]	503	521/600	0.007		GLY[d]	491	507	<0.001
	ACN	498	513	0.001		ACN	494	509	<0.001
	DMSO	503	521	0.002		DMSO	499	524	0.001

[a] Quantum yields (φ_{fl}) were measured by using fluorescein as a reference ($\varphi_{fl}=0.79$ in 0.1 M NaOH). [b] ACN = acetonitrile, PEN = pentadecane, HEX = hexane, GLY = glycerol, and SIO = silicon oil. [c] The data determined in silicon oil/chloroform (90:10, v/v), $\eta=400$ MPa s. [d] The data determined in a glycerol/water mixture (90:10, v/v), $\eta=215$ MPa s.

viscosity solvents and restore their fluorescence intensity in the viscous glycerol. Because the intramolecular rotation is the main pathway to impair the fluorescence emission,[9] their emission intensity would be enhanced in the polar glycerol solution, 2) the second types are BDP-G1 and BDP-G2, which bear three-folded OEG branches and display negligible fluorescence emission in common solvents and show somewhat enhancement in the viscous nonpolar silicon oil. Although the intramolecular rotation is restricted in viscous glycerol, the fluorescence emission might be quenched by other pathways, and 3) BDP-G1-Me shows high quantum yields ($\varphi_{fl}>0.10$) in most of the organic solvents, whereas BDP-G1-CHO exhibits only little detectable fluorescence emission ($\varphi_{fl}<0.01$) in all organic solvents. Therefore, both BDP derivatives showing solvents independence are ascribed to the third types. For BDP-G1-Me, the rotation of the single bond between the benzene moiety and BDP is greatly restricted due to the methyl substituents on the BDP core. Therefore, it is reasonable that BDP-G1-Me show high φ_{fl} values in various solvents.[9a] For BDP-G1-CHO, the intramolecular rotation and the enhanced electron effect might account for its low φ_{fl} value. All the photophysical measurements determined in dilute solution served for the investigation in concentrated aqueous solution at various temperatures, which will be discussed below.

The viscosity-dependent fluorescence intensities of the BDP derivatives were examined by fluorescence spectroscopy. BDP-G0 exhibited a negligible fluorescence intensity in pure water and showed progressively enhancement upon gradually increasing the fraction of glycerol in the solvent mixture (Figure 2a). BDP-G1 demonstrated a similar spectral profile and a moderate intensity enhancement, as shown in Figure 2b. In contrast, BDP-G2 only showed a small intensity enhancement and even a new band in a solution containing a high fraction of glycerol (Figure S1 in the Supporting Information), which is consistent to the pale emission when the volume fraction of glycerol exceeds 80% (Figure S2 in the Supporting Information). The fluorescence enhancement in the viscous glycerol solution was quantitatively verified by the quantum yield φ_{fl} (Figure 3). The φ_{fl} value of BDP-G0 increased dramatically and reached 46% (90 vol% fraction glycerol), which is much higher than those for BDP-G1 (3.3%) and BDP-G2 (0.7%) under the same conditions. Considering that the intramolecular rotation is restricted in the viscous glycerol solution, some other pathways might be responsible for the low φ_{fl} values of BDP-G1 and BDP-G2 in glycerol.

The emission peak at the long-wavelength band for BDP-G2 in a high fraction of glycerol solution might be ascribed to the emission of a charge-transfer excited state (Figure S3b in the Supporting Information).[18] The excitation spectrum revealed that the long-wavelength band is from the BDP maximum absorption (Figure S3a in the Supporting Information). This emission band is strongly dependent on the solvents polarity and viscosity. Considering that the intramolecular rotation is restricted when dissolving BDP-G2 in the viscous glycerol or silicon oil, respectively, we can compare the solvents polarity effect on the emission spectra (Figure S3b in the Supporting Information). The emission spectrum show higher intensity in silicon oil than the one in glycerol without a charge-transfer emission band. Therefore, the charge transfer impaired the quantum yield could be blocked for BDP-G2 in low polarity solvents. In contrast, the fluorescence of BDP-G1 only shows little change in both solvents.

Photoinduced electron transfer (PET) quenches the fluorescence of BDP-G1 and BDP-G2 in viscous glycerol solutions. Due to the electron-donating ability of the OEG substituent, it is plausible that the three-folded OEG dendron donates an electron to the acceptor BDP fluorophore in the excited state, and thus impairing the fluorescence emission.[8a] Figure 4 illustrates the PET process based on the HOMO energy level calculation of both BDP acceptors and benzene moiety donors at the B3LYP/6-31G level. The HOMO level of G1 is calculated to be −5.85 eV, which is higher than that of BDP (−5.97 eV). Therefore, it is plausible that the PET can impair the fluorescence emission of BDP-G1 and BDP-G2 in glycerol. In contrast, the four-methyl-substituted BDP displays higher HOMO level than the BDP without a substituent due to the electron-donating ability of the methyl group (−5.38 eV). Therefore, BDP-G1-Me shows a high φ_{fl} value in various solvents because the PET pathway is not significant. BDP-G1-CHO is expected to exhibit a weak emission due to a strong PET effect (Figure 4b).

The feasibility of the intramolecular PET can be determined by the thermodynamic free energy, which is dependent on the

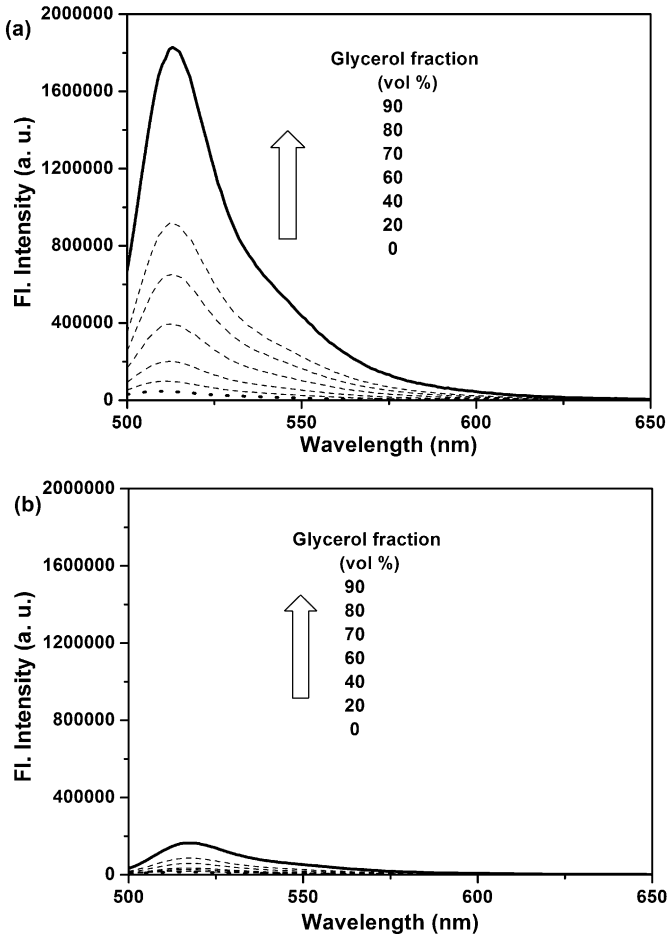

Figure 2. Fluorescence spectra of a) BDP-G0 and b) BDP-G1 in glycerol/water mixtures with different fractions of glycerol, the concentration of the BDP derivatives was 2.0 μM. The dotted and solid lines were acquired in pure water and a glycerol/water mixture (9:1, v/v). λ_{ex} = 490 nm.

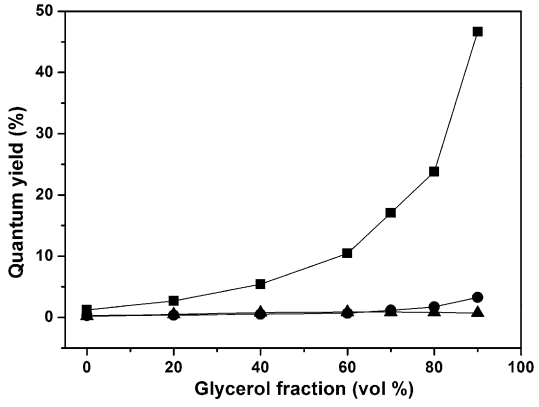

Figure 3. Plots of the quantum yield versus the glycerol fraction for the BDP derivatives (■ = BDP-G0, ● = BDP-G1, and ▲ = BDP-G2) in glycerol/water mixtures.

polarity of the solvents. According to the Rehm–Weller equation [Eq. (1)],[19] the free energy of a PET can be estimated by the comparison of the redox potentials of both the BDP fluorophore and the benzene moiety.

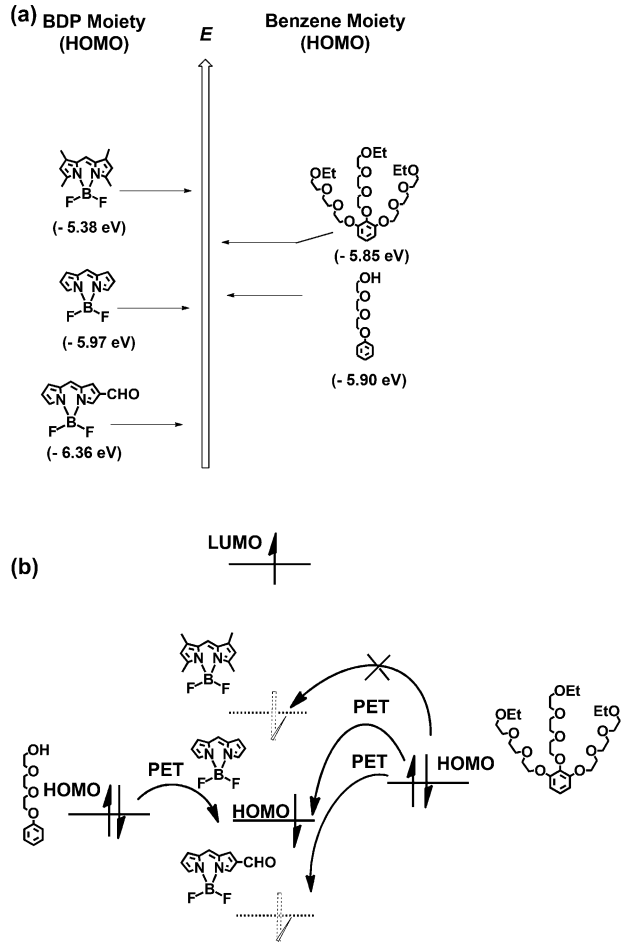

Figure 4. a) HOMO level of the BDP fluorophore and the benzene moieties. b) Schematic PET process in dilute solution.

$$\Delta G_{PET} = E_{ox(d)} - E_{red(a)} - E_{0,0} - (e^2/\varepsilon d) \quad (1)$$

Where ΔG_{PET} is the Gibbs free energy of the PET, $E_{ox(d)}$ and $E_{red(a)}$ are the oxidation potential of the benzene moieties and the reduction potential of the BDP, respectively, $E_{0,0}$ is the excitation energy of the BDP fluorophore, ε is the dielectric constant of the solvent, and d is the distance between the charges in the separated state.

Nagano and coworkers has demonstrated that, with the polarity of solvents increasing, the oxidation potential of the benzene moiety decreased and the reduction potential of the BDP increased.[8a] The $E_{0,0}$ values show a negligible change in the various solvents (except for BDP-G1-CHO), whereas the last term, $e^2/\varepsilon d$, is usually too small to be taken into consideration. Therefore, a PET from the donor moiety to the acceptor BDP is favored due to the decreased free energy in high polarity solvents, which accounts for our observation that both BDP-G1 and BDP-G2 display low quantum yield in polar glycerol solution.

Spectroscopic properties of the BDP derivatives in aqueous solution

There is a delicate balance for molecules to have thermoresponsive properties. BDP-G1, BDP-G1-TEG, and BDP-G2 are thermoresponsive, that is, these above-mentioned BDP derivatives are water soluble at low temperature and their aqueous solutions turn into opaque at elevated temperatures. Taking BDP-G1 as an example, due to the dehydration and hydration of OEG groups, the transparent yellow solution at room temperature (25 °C) turned turbid after heating (50 °C) and changed back after cooling (Figure 5). This thermoresponsive process is reversible and could be repeated for multiple times. In contrast, the aqueous solutions of BDP-G0, BDP-G1-Me, and BDP-G1-CHO are not thermoresponsive.

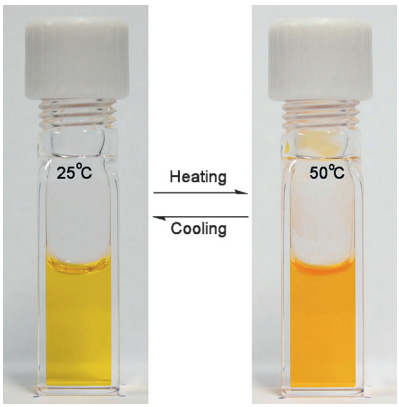

Figure 5. Aqueous solution of BDP-G1 (0.04 wt%) at 25 and 50 °C.

Turbidity tests were performed by UV/Vis measurements to investigate the thermoresponsive behavior of BDP-G1 and BDP-G2 in detail (for BDP-G1-TEG, see the Supporting Information). As shown in Figure 6, the turbidity curves plotted temperatures were assembled and the apparent phase transition temperatures (T_{cp}s) (the temperature reached at 50% of the initial transmittance at $\lambda = 700$ nm) plotted concentrations were compared. Regarding the thermoresponsive properties, there are two important points worthy of note: 1) The T_{cp} values are concentration dependent. As the concentration of BDP-G1 decreased from 0.12 to 0.04 wt%, the T_{cp} values significantly increased from 19 to 37 °C, accompanied by a broader phase-transition range. In contrast, BDP-G2 only shows six degree changes in the same concentration range. We presume that the overall hydrophilicity for small molecules BDP-G1 will be influenced much more than that of BDP-G2 by concentration. 2) The T_{cp} values are generation dependent. Besides the smaller T_{cp} value changes, BDP-G2 showed a much higher T_{cp} value than BDP-G1 at the same concentration, which could be ascribed to the high hydrophilicity of the G2 dendron (Figure S5 in the Supporting Information).

It is more interesting that BDP-G1, BDP-G1-TEG, and BDP-G2 behave as heat-induced fluorescence thermometers. Both BDP-G1 and BDP-G2 showed very faint fluorescence when the temperature was lower than their T_{cp} values but presented drastic fluorescence emission after heating (Figures S10a and b in the Supporting Information). The color of their solution changed from green to yellow (under $\lambda = 365$ nm UV excitation). In contrast, BDP-G1-TEG did not show too much changes in brightness as well as color during the heating process (Figure S10c in the Supporting Information). The photophysical properties from the apparent emission intensity and the color of the solutions might be ascribed to the different molecule structure and the excited molecules reactivity during the heating process.

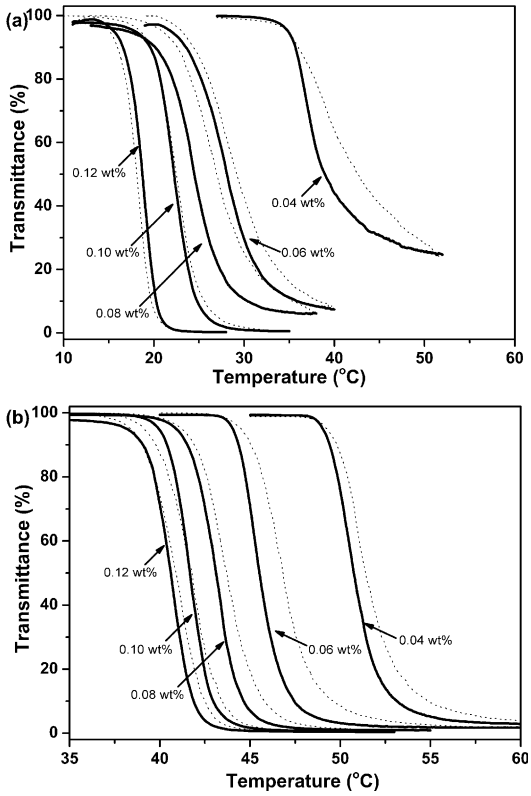

Figure 6. Plots of the transmittance versus the temperature for aqueous solutions of a) BDP-G1 and b) BDP-G2. Heating (solid lines) and cooling (dotted lines) rate is 0.2 K min^{-1}.

The photophysical properties during the thermoresponsive process were monitored by fluorescence spectra at various temperatures. The emission intensities of BDP-G1 and BDP-G2 increased by 22- and 61-fold at their corresponding maximum bands, respectively (Figures 7a and b). As described in the previous studies, two pathways, intramolecular rotation and PET, could quench the fluorescence emission of BDP-G1 and BDP-G2 in dilute solution. The increased microviscosity during the heating process might suppress the free rotation between the dipyrromethane framework and the *meso*-phenyl ring.[9] That is, the hydrophobic BDP fluorophore that stays in a free rotation state at low temperature ($< T_{cp}$) would be wrapped by the dehydrated OEG groups at high temperature ($> T_{cp}$). Thus, the intramolecular rotation is restricted.[2c] In addition, the hydrophilic microenvironment around the BDP fluorophore would change to be hydrophobic due to the dehydration of the OEG

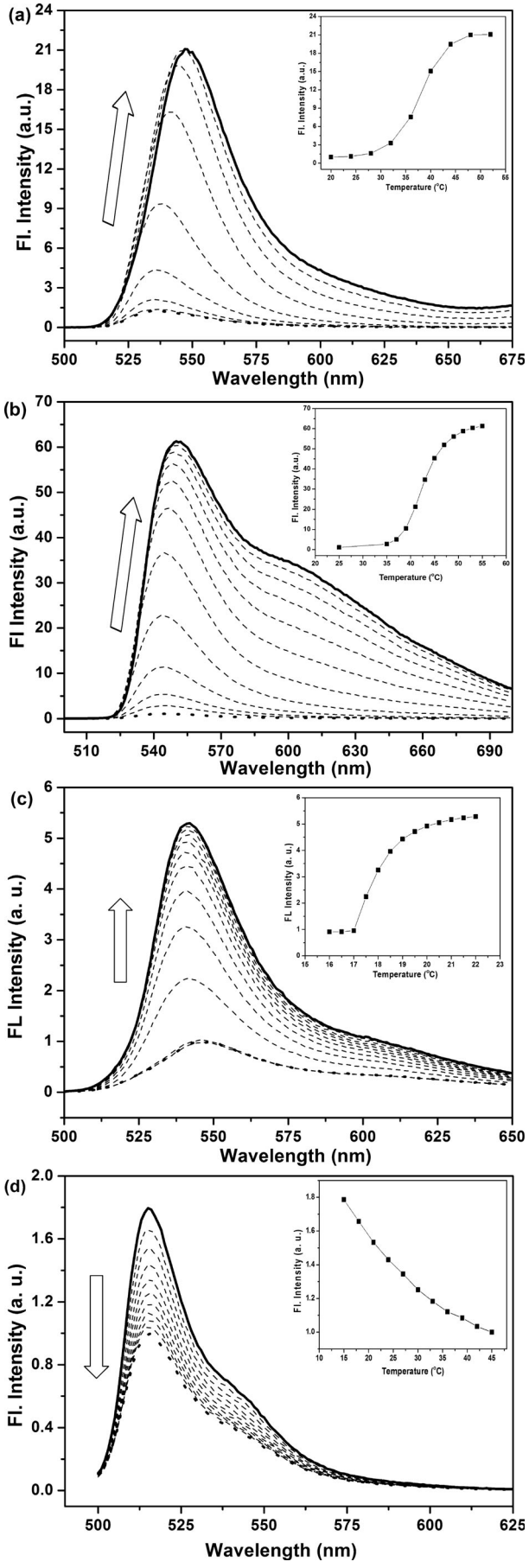

Figure 7. Temperature-varied fluorescence spectra of a) BDP-G1 ($c = 4.14 \times 10^{-4}$ M), b) BDP-G2 ($c = 4.06 \times 10^{-4}$ M), c) BDP-G1-TEG ($c = 3.41 \times 10^{-4}$ M), and d) BDP-G1-Me ($c = 4.00 \times 10^{-4}$ M). The insets are plots of fluorescence intensity at a) 547, b) 550, c) 541, and d) 516 nm versus temperature. $\lambda_{ex} = 490$ nm.

groups after heating.[16d] That is, the polarity around the BDP is greatly decreased. Thus, the PET pathway is impaired.[8a] Both effects work in concert to restore the fluorescence emission of BDP-G1 and BDP-G2 during the heating process.

Noteworthy to mention here is that the emission bands of both molecular thermometers in the locally excited state (LE) undergo bathochromic shifts during the heating process. BDP-G1 underwent a bathochromic shift of 13 nm from 535 to 548 nm, whereas BDP-G2 showed a bathochromic shift of 7 nm (see the Supporting Information), which is attributed to the donor–acceptor interaction between the benzene moieties and the BDP fluorophore during the heating process in polar aqueous solution.[20] In addition, there is a new emission band at long wavelength (around $\lambda = 600$ nm) observed for BDP-G2 after the temperature exceeded 45 °C. This new band is attributed to the TICT state, which is well reported in the BDP derivatives containing an electron donor and an electron acceptor connected by a single bond (Scheme 3).[11,20] An aqueous

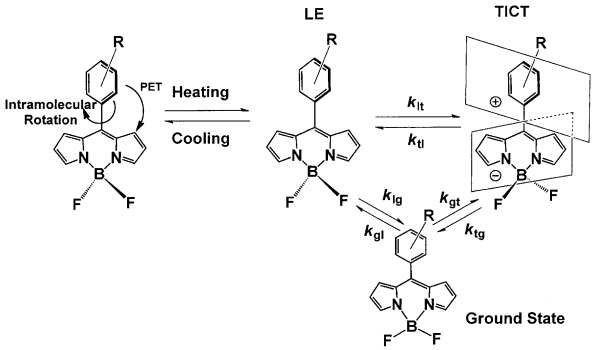

Scheme 3. Photophysical processes for an aqueous solution of BDP-G2.

solution of BDP-G1 did not show the long-wavelength emission band form a TICT state after heating, this might be attributed to the dehydrated OEG branches, which cannot stabilized the TICT state. In contrast, BDP-G1-TEG shows less intensity enhancement (about five-fold) during the thermoresponsive process, accompanied with a little change at the emission maximum (Figure 7c). Therefore, the three-folded OEG branches behaved as electron-donor account for both the emission shift and the intensity enhancement. Motivated by these results, we determined the fluorescence properties of the model compounds BDP-G1-Me (Figure 7d) and BDP-G1-CHO (Figure S12 in the Supporting Information) in concentrated aqueous solution ($c = 4.00 \times 10^{-4}$ M) at different temperatures. Their emission intensities decreased during heating process.

Bioimaging

BDP-G*n* ($n=0$, 1, and 2) show little toxicity as determined by using a standard methyl thiazolyl tetrazolium (MTT, Sigma–Aldrich) assay in HeLa cell lines. HeLa cells were incubated with the BDP derivatives up to 50 μM in phosphate-buffered saline (PBS). Over the course of the test, no apparent toxicity of the BDP derivatives was observed based on no significant differences in the cell morphologies, which is in agreement with a previous report that the BDP sensors have good chemical stability and generally low toxicity.[13] As shown in Figure S13 in the Supporting Information, the cellular viabilities were determined to be higher than 80% after 24 h incubation (except for BDP-G2 at 50 μM). Therefore, the toxicity of the BDP derivatives at low micromolar loading concentrations ($\leq$10 μM) is insignificant over the time scale of the imaging tests.

A practical application of the BDP derivatives in live HeLa cells bioimaging was developed by LSFM. The untreated HeLa cells displayed negligible background fluorescence. The cells were first incubated in the PBS in the presence of BDP-G*n* ($n=$ 0, 1, and 2) for 30 min or 4 h. After replacement of the media to remove the extracellular probe molecules, the cells were studied under LSFM. Interestingly, BDP-G0 showed very strong intracellular fluorescence (Figure 8b). The overlay of a bright-field image and the confocal luminescence showed that the luminescence is localized in the cytoplasm, not in the nucleus or the cell membrane (Figure 8c). In contrast, BDP-G1 and BDP-G2 displayed weak and almost no intracellular fluorescence, respectively. (Figures 8e and h) Therefore, the intracellular fluorescence intensity shows the same tendency as that in glycerol/water mixtures, that is, the high generation dendron impairs the fluorescence intensity in live cells. Two possibilities may account for the fluorescence difference: 1) BDP-G1 and BDP-G2 might have a poor cell permeability due to an increased size of the dendrons, whereas BDP-G0 passed the cell membrane smoothly due to its smaller size. 2) The fluorescence intensities of the BDP derivatives followed the above order are attributable to their lipophilicity, sensor BDP-G0 with high lipophilicity preferentially localizes in hydrophobic domains of cellular organelles. The first possibility is excluded due to the observation that the fluorescent BDP dyes with branched tri(ethylene glycol) arms still show a strong fluorescence intensity in cells.[14,21] BDP-G0 is likely to stay in the endocytotic vesicles and to show enhanced fluorescence intensity in this confined environments.[9a]

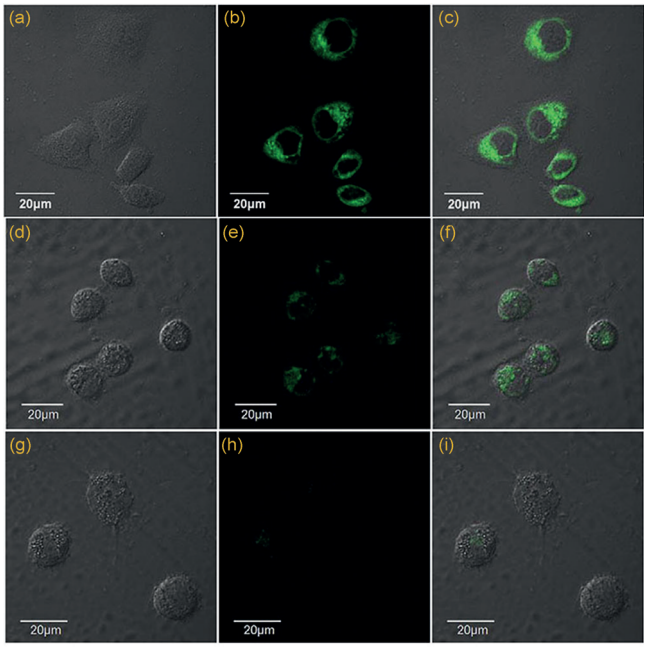

Figure 8. a,d,g) Bright-field images and b,e,h) confocal luminescence of HeLa cells incubated with BDP-G0, BDP-G1, and BDP-G2 in PBS for 30 min at 25 °C. c,f,i) Overlay images of the bright-field and the confocal images.

Conclusion

In summary, amphiphilic BDP derivatives with different hydrophilic substituents were successfully prepared. BDP-G1, BDP-G1-TEG, and BDP-G2 displayed thermoresponsive properties and enhanced fluorescence intensities after heating. This is the first report referred to thermoresponsive dendrimers of which the fluorescence intensity could be enhanced at elevated temperature. Detailed investigations revealed that intramolecular rotation and PET quench pathway were impaired in the heating process. Furthermore, these compounds were used in aqueous solutions as luminescent dyes for imaging in living HeLa cells. The hydrophilic dendrons were needed for the solubility in aqueous solution, whereas lipophilic BDP-G0 permeated the cells with ease. Therefore, preliminary cell image studies revealed that the intracellular fluorescence intensity is lipophilicity dependent. Further applications of other fluorescent probes in cell imaging are underway and will be reported in due course.

Experimental Section

Materials

Trifluoroacetic acid was purchased from ACROS. Pyridinium chlorochromate (PCC), pyrrole, *p*-chloranil, boron trifluoride diethyl etherate ($BF_3{\cdot}OEt_2$) were purchased from TCI. Dichloromethane and 1,2-dichloroethane was dried over CaH_2. Tetrahydrofuran (THF) was predried over sodium and then heated to reflux over $LiAlH_4$ before use. Triethylamine was dried over sodium hydroxide (NaOH) pellets. Other reagents and solvents were purchased at reagent grade and used without further purification. All synthetic steps were run under a nitrogen atmosphere. Macherey–Nagel precoated thin-layer chromatography (TLC) plates (silica gel 60 G/UV254, 0.25 mm) were used for analysis. Silica gel 60M (Macherey–Nagel, 0.040–0.063 mm, 200–300 mesh) was used as the stationary phase for column chromatography. All samples were dried thoroughly under vacuum prior to analytical measurements to remove strongly adhering solvent molecules.

General instrumentation and measurements

^1H and ^{13}C NMR spectra were recorded on a Bruker AV 500 (^1H: 500 MHz, ^{13}C: 125 MHz) spectrometer, and chemical shifts are re-

ported as δ values in [ppm] relative to internal tetramethylsilane (Me_4Si). High-resolution MALDI/TOF MS analyses were performed on Ionspec Ultra instruments. UV/Vis turbidity measurements were carried out on a PE UV/Vis spectrophotometer (Lambda 35) equipped with a thermo-controlled bath. An aqueous solution of the sensor was placed in the spectrophotometer (path length 1 cm) and heated or cooled at a rate of 0.2 K min^{-1}. The absorptions of the solution at $\lambda = 700$ nm were recorded every 5 s. The cloud point (T_{cp}) is determined as the one at which the transmittance at $\lambda = 700$ nm has reached 50% of its initial value. The fluorescence spectra were measured on Horiba Jobin Yvon Fluorolog-3 equipped with a Peltier temperature controller. Confocal imaging of cells was performed with a modified Olympus FV1000 laser scanning confocal microscope equipped a continuous-wave NIR laser operating at $\lambda = 980$ nm (Connet Fiber Optics, China). The viscosity was determined at a speed of 75 revolutions per minute by the DV-79 Series digital viscometer (Shanghai Nirun Intelligent Technology Co., Ltd. China).

Synthesis

BDP-G1

A solution of *p*-chloranil (0.41 g, 1.65 mmol) in dichloromethane (10 mL) was added dropwise to a solution of the corresponding aldehyde (1.24 g, 1.65 mmol, Scheme S1 in the Supporting Information) in dichloromethane (20 mL) at $-5\,^{\circ}C$. The reaction mixture was stirred at $-5\,^{\circ}C$ for 30 min and then the temperature was risen to RT. The mixture was stirred at RT for another 13 h before triethylamine (TEA) (5.00 g, 49.41 mmol) and $BF_3{\cdot}OEt_2$ (7.00 g, 49.32 mmol) were added. The solution was stirred at RT for 5 h before partitioned between brine and dichloromethane. The organic portion was dried over $MgSO_4$ before concentration in vacuo. The residue was purified on a silica column by using dichloromethane/MeOH (from 50:1 to 30:1) as the eluent to afford compound BDP-G1 as an orange viscous liquid (0.90 g, 69% over two steps). ^{1}H NMR ($CDCl_3$): $\delta = 1.17$–1.21 (m, 9H; CH_3), 3.47–3.75 (m, 30H; CH_2), 3.83–3.88 (m, 6H; CH_2), 4.18 (t, $J = 4.7$ Hz, 4H; CH_2), 4.27 (t, $J = 4.9$ Hz, 2H; CH_2), 6.54–6.56 (m, 2H; pyrrole-H), 6.83 (s, 2H; CH), 7.01 (d, $J = 4.1$ Hz, 2H; pyrrole-H), 7.92 ppm (s, 2H; pyrrole-H); ^{13}C NMR ($CDCl_3$): $\delta = 8.77$, 15.10, 47.34, 66.55, 66.57, 69.11, 69.61, 69.71, 69.74, 70.50, 70.55, 70.59, 70.61, 70.76, 72.58, 110.57, 118.52, 128.52, 131.53, 134.69, 140.80, 143.87, 147.02, 152.48 ppm; HRMS (MALDI/TOF): *m/z* calcd for $C_{39}H_{59}BN_2O_{12}F_2Na$: 818.4066 $[M+Na]^+$; found 818.4057.

BDP-G1-Me

BDP-G1-Me was isolated as an orange solid (0.89 g, 55%). ^{1}H NMR (CD_2Cl_2): $\delta = 1.14$–1.19 (m, 9H; CH_3), 1.54 (s, 6H; CH_3), 2.50 (s, 6H; CH_3), 3.45–3.83 (m, 36H; CH_2), 4.12 (s, 4H; CH_2), 4.22 (s, 2H; CH_2), 6.02 (s, 2H; pyrrole-H), 6.57 ppm (s, 2H; CH). ^{13}C NMR (CD_2Cl_2): $\delta =$ 8.64, 14.10, 14.29, 14.95, 47.43, 66.40, 68.87, 69.50, 69.65, 69.70, 70.37, 70.52, 70.53, 70.64, 72.64, 107.13, 121.08, 129.90, 131.24, 141.39, 143.35, 153.55, 155.45 ppm; HRMS (MALDI/TOF): *m/z* calcd for $C_{43}H_{67}BN_2O_{12}F_2Na$: 874.4692 $[M+Na]^+$; found 874.4683.

BDP-G0

The synthesis of BDP-G0 was started from the reported aldehyde[17] and isolated as an orange viscous liquid (0.65 g, 45%). ^{1}H NMR ($CDCl_3$): $\delta = 3.56$–3.60 (m, 1H; OH), 3.63–3.65 (m, 2H; CH_2), 3.72–3.77 (m, 4H; CH_2), 3.93 (t, $J = 4.7$ Hz, 2H; CH_2), 4.24 (t, $J = 4.7$ Hz, 2H; CH_2), 6.54–6.56 (m, 2H; pyrrole-H), 6.97 (d, $J = 4.1$ Hz, 2H; pyrrole-H), 7.07 (d, $J = 8.8$ Hz, 2H; CH), 7.53 (d, $J = 8.8$ Hz, 2H; CH), 7.92 ppm (s, 2H; pyrrole-H); ^{13}C NMR ($CDCl_3$): $\delta = 61.71$, 67.64, 69.53, 70.31, 70.86, 72.54, 114.67, 118.31, 126.50, 131.40, 132.41, 134.81, 143.41, 147.37, 161.25 ppm; HRMS (MALDI/TOF): *m/z* calcd for $C_{21}H_{23}BN_2O_4F_2Na$: 438.1656 $[M+Na]^+$; found 438.1647.

BDP-G2

BDP-G2 was isolated as an orange viscous liquid (0.30 g, 49% over two steps). ^{1}H NMR (CD_2Cl_2): $\delta = 1.14$–1.18 (m, 27H; CH_3), 3.45–3.86 (m, 144H; CH_2), 4.08–4.27 (m, 24H; CH_2), 4.41 (d, $J = 12.4$ Hz, 6H; CH_2), 6.58 (d, $J = 6.6$ Hz, 8H; CH), 6.87 (s, 2H; pyrrole-H), 7.07 (d, $J =$ 3.8 Hz, 2H; pyrrole-H), 7.90 ppm (s, 2H; pyrrole-H); ^{13}C NMR (CD_2Cl_2): $\delta = 15.00$, 66.38, 68.66, 69.10, 69.46, 69.49, 69.63, 69.68, 69.79, 69.81, 70.41, 70.50, 70.52, 70.56, 70.57, 70.59, 70.65, 70.70, 70.76, 72.28, 72.62, 73.00, 73.04, 106.68, 110.43, 118.53, 128.78, 131.62, 134.01, 134.75, 137.45, 140.78, 143.77, 147.25, 152.54 ppm; HRMS (MALDI/TOF): *m/z* calcd for $C_{126}H_{209}BN_2O_{48}F_2Na$: 2589.3960 $[M+Na]^+$; found 2589.3964.

BDP-G1-TEG

BDP-G1-TEG was isolated as an orange viscous liquid (20 mg, 10%). ^{1}H NMR ($CDCl_3$): $\delta = 1.20$ (t, $J = 6.3$ Hz, 9H; CH_3), 3.51–3.92 (m, 46H; CH_2), 4.14 (s, 6H; CH_2), 4.45 (s, 2H; CH_2), 6.55 (d, $J =$ 13.8 Hz, 4H; CH), 6.96 (s, 2H; pyrrole-H), 7.05 (d, $J = 7.8$ Hz, 2H; CH), 7.53 (d, $J = 7.7$ Hz, 2H; pyrrole-H),7.91 ppm (s, 2H; pyrrole-H); ^{13}C NMR ($CDCl_3$): $\delta = 15.18$, 27.21, 29.32, 29.52, 29.55, 29.62, 29.70, 29.78, 31.91, 55.07, 66.66, 67.92, 68.91, 69.40, 69.64, 69.84, 70.57, 70.59, 70.73, 70.61, 70.87, 70.95, 72.37, 73.30, 74.89, 107.30, 114.71, 118.30, 118.32, 126.47, 131.39, 132.41, 133.75, 134.83, 137.83, 143.43, 147.40, 152.63, 161.35 ppm; HRMS (MALDI/TOF): *m/z* calcd for $C_{52}H_{77}BN_2O_{16}F_2Na$: 1056.5267 $[M+Na]^+$; found 1056.5262.

BDP-G1-CHO

$POCl_3$ (1 mL) was added dropwise to a vigorously stirred anhydrous solution of DMF (1 mL) which was kept in an ice bath under N_2. The resulting pale yellow viscous liquid was allowed to stir at room temperature for additional 30 min. To this, a solution of BDP-G1 (440 mg, 0.55 mmol) in 1,2-dichloroethane (30 mL) was then slowly introduced and the resultant brown solution was heated at 60 °C for 3 h. The reaction mixture was cooled to RT and poured into an ice-cold saturated $NaHCO_3$ solution and stirred for 1 h. This mixture was extracted with dichloromethane (2×100 mL) and dried over anhydrous Na_2SO_4. The solvent was evaporated in vacuo. The residue was purified on a silica column by using dichloromethane/MeOH (from 100:1 to 70:1) as the eluent to afford compound BDP-G1-CHO as an orange viscous liquid (0.35 g, 78%). ^{1}H NMR ($CDCl_3$): $\delta = 1.16$–1.21 (m, 9H; CH_3), 3.48–3.88 (m, 36H; CH_2), 4.20 (s, 4H; CH_2), 4.30 (s, 2H; CH_2), 6.72 (s, 1H; pyrrole-H), 6.84 (s, 2H; CH), 7.22 (s, 1H; pyrrole-H), 7.37 (s, 1H; pyrrole-H), 8.14 (s, 1H; pyrrole-H), 8.26 (s, 1H; pyrrole-H), 9.87 ppm (s, 1H; CH); ^{13}C NMR ($CDCl_3$): $\delta =$ 15.24, 66.72, 66.75, 69.50, 69.84, 69.88, 69.94, 70.76, 70.80, 70.81, 70.97, 72.90, 76.90, 77.15, 77.41, 110.95, 121.49, 128.04, 128.83, 131.87, 134.55, 135.05, 135.12, 135.14, 136.83, 141.85, 142.72, 149.14, 149.27, 152.89, 184.97 ppm; HRMS (MALDI/TOF): *m/z* calcd for $C_{40}H_{59}BN_2O_{13}F_2Na$: 846.4019 $[M+Na]^+$; found 846.4006.

Quantum yield of the fluorescence

Fluorescence quantum yields were determined by a relative method by using a solution of fluorescein ($\varphi_s = 0.79$, 0.1 M NaOH) as a reference.[22] The excitation wavelength was $\lambda = 490$ nm. The

fluorescence quantum yields were calculated based on Equation (2).

$$\varphi_x = \varphi_s \times (A_s F_x n_x^2)/(A_x F_s n_s^2) \quad (2)$$

where A_s and A_x are the absorbance values of the reference and samples solutions at their respective excitation wavelengths, F_s and F_x are the corresponding integrated fluorescence intensities, and n is the refractive index of the solvent of the samples (n_x) or of the reference (n_s). The absorbance of the samples and the references at their respective excitation wavelengths was kept below 0.1. The refractive index of the glycerol/water solvent of the sample (n_x) was calculated according to Equation (3).[23]

$$n_x = n_s + [0.0011625 \times \text{glycerol}(\text{m m}^{-1}\,\%) \times \rho] \quad (3)$$

where ρ is specific gravity of glycerol.

Cytotoxicity of the BDP derivatives

The cytotoxicity was measured by performing methyl thiazolyl tetrazolium (MTT) assays on the HeLa cells lines, which were provided by the Institute of Biochemistry and Cell Biology (Chinese Academy of Sciences). The HeLa cells were grown in RPMI 1640 (Roswell Park Memorial Institute's Medium) supplemented with 10% FBS (fetal bovine serum) at 37 °C under 5% CO_2. The BDP derivatives at 10, 20, 30, 40, and 50 μM concentration were added to the wells of the treatment group. The cells were incubated for 24 h at 37 °C under 5% CO_2 and then MTT was added to the wells for test.

Live cell imaging

HeLa cells were placed on 14 mm glass coverslips and allowed to adhere for 12 h. The cells were washed with PBS and then incubated solely with BDP-G0, BDP-G1, and BDP-G2 in PBS (pH 7.4) at 25 °C for 30 min, 4 h and 4 h, respectively. Cell imaging was then carried out after washing the cells with PBS. The excitation wavelength is $\lambda = 488$ nm, and the emission wavelength is $\lambda = 500$–600 nm.

Computational methods

All gas-phase calculations were carried out by using Gaussian 09 suite of programs.[24] The B3LYP[25] hybrid functional in conjunction with the 6-31G(d) basis set[26] is utilized to optimize all geometries fully and to perform the harmonic vibrational analyses for confirming minima (all real frequencies).

Acknowledgements

This work was financially supported by the National Natural Science Foundation of China (Nos. 21034004, 21204047, and 21374058). We thank Prof. Afang Zhang (Shanghai University), Prof. Anjun Qin (South China University of Technology), and Prof. Xiaohua Chen (Chongqing University) for their help, and Dr. Hongmei Deng for her assists with the NMR measurements.

Keywords: BODIPY · dendrimers · fluorescence · imaging agents · thermoresponsiveness

[1] C. Pietsch, U. S. Schubert, R. Hoogenboom, *Chem. Commun.* **2011**, *47*, 8750–8765.
[2] a) K. Okabe, N. Inada, C. Gota, Y. Harada, T. Funatsu, S. Uchiyama, *Nat. Commun.* **2012**, *3*, 1–9; b) T. Tsuji, S. Yoshida, A. Yoshida, S. Uchiyama, *Anal. Chem.* **2013**, *85*, 9815–9823; c) D. P. Wang, R. Miyamoto, Y. Shiraishi, T. Hirai, *Langmuir* **2009**, *25*, 13176–13182.
[3] Y. Hiruta, M. Shimamura, M. Matsuura, Y. Maekawa, T. Funatsu, Y. Suzuki, E. Ayano, T. Okano, H. Kanazawa, *ACS Macro Lett.* **2014**, *3*, 281–285.
[4] C. Y. Chen, C. T. Chen, *Chem. Commun.* **2011**, *47*, 994–996.
[5] R. R. Ramireddy, K. R. Raghupathi, D. A. Rorres, S. Thayumanavan, *New J. Chem.* **2012**, *36*, 340–349.
[6] a) D. W. Chang, L. M. Dai, *J. Mater. Chem.* **2007**, *17*, 364–371; b) D. W. Chang, I.-Y. Jeon, J.-B. Baek, L. M. Dai, *Chem. Commun.* **2010**, *46*, 7924–7926; c) D. W. Chang, H.-J. Choi, S.-M. Jung, L. M. Dai, J.-B. Baek, *J. Mater. Chem.* **2012**, *22*, 13365–13373.
[7] a) A. Loudet, K. Burgess, *Chem. Rev.* **2007**, *107*, 4891–4932; b) G. Ulrich, R. Ziessel, A. Harriman, *Angew. Chem.* **2008**, *120*, 1202–1219; *Angew. Chem. Int. Ed.* **2008**, *47*, 1184–1201; c) N. Boens, V. Leen, W. Dehaen, *Chem. Soc. Rev.* **2012**, *41*, 1130–1172; d) L. Yuan, W. Lin, K. Zheng, L. He, W. Huang, *Chem. Soc. Rev.* **2013**, *42*, 622–661; e) M. Baruah, W. Qin, N. Basarić, W. M. D. Borggraeve, N. Boens, *J. Org. Chem.* **2005**, *70*, 4152–4157; f) M. Benstead, G. A. Rosser, A. Beeby, G. H. Mehl, R. W. Boyle, *Photochem. Photobiol. Sci.* **2011**, *10*, 992–999.
[8] a) H. Sunahara, Y. Urano, H. Kojima, T. Nagano, *J. Am. Chem. Soc.* **2007**, *129*, 5597–5604; b) Y. Gabe, Y. Urano, K. Kikuchi, H. Kojima, T. Nagano, *J. Am. Chem. Soc.* **2004**, *126*, 3357–3367; c) T. Matsumoto, Y. Urano, T. Shoda, H. Kojima, T. Nagano, *Org. Lett.* **2007**, *9*, 3375–3377; d) M. Isik, T. Ozdemir, I. S. Turan, S. Kolemen, E. U. Akkaya, *Org. Lett.* **2013**, *15*, 216–219; e) J. J. Shie, Y. C. Liu, Y. M. Lee, C. Lim, J. M. Fang, C. H. Wong, *J. Am. Chem. Soc.* **2014**, *136*, 9953–9961.
[9] a) M. K. Kuimova, G. Yahioglu, J. A. Levitt, K. Suhling, *J. Am. Chem. Soc.* **2008**, *130*, 6672–6673; b) I. López-Duarte, T. T. Vu, A. Izquierdo, J. A. Bull, M. K. Kuimova, *Chem. Commun.* **2014**, *50*, 5282–5284; c) Z. G. Yang, Y. X. He, J. H. Lee, N. Park, M. Suh, W. S. Chae, J. F. Cao, X. J. Peng, H. Jung, C. Kang, J. S. Kim, *J. Am. Chem. Soc.* **2013**, *135*, 9181–9185; d) M. A. H. Alamiry, A. C. Benniston, G. Copley, K. J. Elliott, A. Harriman, B. Stewart, Y.-G. Zhi, *Chem. Mater.* **2008**, *20*, 4024–4032.
[10] L. Wang, Y. Xiao, W. M. Tian, L. Z. Deng, *J. Am. Chem. Soc.* **2013**, *135*, 2903–2906.
[11] a) E. Lager, J. Liu, A. Aguilar-Aguilar, B. Z. Tang, E. Peña-Cabrera, *J. Org. Chem.* **2009**, *74*, 2053–2058; b) Y. Hong, J. W. Y. Lam, B. Z. Tang, *Chem. Commun.* **2009**, 4332–4353; c) R. R. Hu, E. Lager, A. Aguilar-Aguilar, J. Z. Liu, J. W. Y. Lam, H. H. Y. Sung, I. D. Williams, Y. C. Zhong, K. S. Wong, E. Peña-Cabrera, B. Z. Tang, *J. Phys. Chem. C* **2009**, *113*, 15845–15853.
[12] a) R. París, I. Quijada-Garrido, O. García, M. Liras, *Macromolecules* **2011**, *44*, 80–86; b) A. Nagai, K. Kokada, J. Miyake, Y. Cyujo, *J. Polym. Sci. Part A* **2010**, *48*, 627–634; c) M. Liras, J. M. Carcía-García, I. Quijada-Garrida, A. Gallardo, R. París, *Macromolecules* **2011**, *44*, 3739–3745.
[13] S. Li, K. Liu, G. C. Kuang, T. Masuda, A. Zhang, *Macromolecules* **2014**, *47*, 3288–3296.
[14] S. Atilgan, Z. Ekmekci, A. L. Dogan, D. Guc, E. U. Akkaya, *Chem. Commun.* **2006**, 4398–4400.
[15] a) S. L. Zhu, J. T. Zhang, G. K. Vegesna, F.-T. Luo, S. A. Green, H. Y. Liu, *Org. Lett.* **2011**, *13*, 438–441; b) S. L. Zhu, J. T. Zhang, G. K. Vegesna, R. Pandey, F.-T. Luo, S. A. Green, H. Y. Liu, *Chem. Commun.* **2011**, *47*, 3508–3510; c) S. L. Zhu, J. G. Zhang, G. Vegesna, A. Tiwari, F.-T. Luo, M. Zeller, R. Luck, H. H. Li, S. Green, H. Y. Liu, *RSC Adv.* **2012**, *2*, 404–407.
[16] a) W. Li, A. Zhang, K. Feldman, P. Walde, A. D. Schlüter, *Macromolecules* **2008**, *41*, 3659–3667; b) W. Li, A. Zhang, A. D. Shclüter, *Chem. Commun.* **2008**, 5523–5525; c) W. Li, D. L. Wu, A. D. Schlüter, A. Zhang, *J. Polym. Sci. Part A* **2009**, *47*, 6630–6640; d) M. J. N. Junk, W. Li, A. D. Schlüter, G. Wegner, H. W. Spiess, A. Zhang, D. Hinderberger, *Angew. Chem.* **2010**, *122*, 5818–5823; *Angew. Chem. Int. Ed.* **2010**, *49*, 5683–5687.
[17] W. Wang, A. D. Q. Li, *Bioconjugate Chem.* **2007**, *18*, 1036–1052.
[18] a) M. Kollmannsberger, K. Rurack, U. Resch-Genger, J. Daub, *J. Phys. Chem. A* **1998**, *102*, 10211–10220; b) K. Rurack, M. Kollmannsberger, U. Resch-Genger, J. Daub, *J. Am. Chem. Soc.* **2000**, *122*, 968–969.
[19] D. Rehm, A. Well, *Isr. J. Chem.* **1970**, *8*, 259–271.
[20] Z. R. Grabowski, K. Rotkiewicz, W. Rettig, *Chem. Rev.* **2003**, *103*, 3899–4301.

[21] G. K. Vegesna, S. R. Sripathi, J. T. Zhang, S. T. Zhu, W. L. He, F.-T. Luo, W. J. Jahng, M. Frost, H. Y. Liu, *ACS Appl. Mater. Interfaces* **2013**, *5*, 4107.
[22] J. Q. Umberger, V. K. LaMer, *J. Am. Chem. Soc.* **1945**, *67*, 1099 – 1109.
[23] D. Basker, *Analyst* **1978**, *103*, 185 – 186.
[24] Gaussian 09, Revision D.01, M. J. Frisch, G. W. Trucks, H. B. Schlegel, G. E. Scuseria, M. A. Robb, J. R. Cheeseman, G. Scalmani, V. Barone, B. Mennucci, G. A. Petersson, H. Nakatsuji, M. Caricato, X. Li, H. P. Hratchian, A. F. Izmaylov, J. Bloino, G. Zheng, J. L. Sonnenberg, M. Hada, M. Ehara, K. Toyota, R. Fukuda, J. Hasegawa, M. Ishida, T. Nakajima, Y. Honda, O. Kitao, H. Nakai, T. Vreven, J. A. Montgomery, Jr., J. E. Peralta, F. Ogliaro, M. Bearpark, J. J. Heyd, E. Brothers, K. N. Kudin, V. N. Staroverov, R. Kobayashi, J. Normand, K. Raghavachari, A. Rendell, J. C. Burant, S. S. Iyengar, J. Tomasi, M. Cossi, N. Rega, J. M. Millam, M. Klene, J. E. Knox, J. B. Cross, V. Bakken, C. Adamo, J. Jaramillo, R. Gomperts, R. E. Stratmann, O. Yazyev, A. J. Austin, R. Cammi, C. Pomelli, J. W. Ochterski, R. L. Martin, K. Morokuma, V. G. Zakrzewski, G. A. Voth, P. Salvador, J. J. Dannenberg, S. Dapprich, A. D. Daniels, O. Farkas, J. B. Foresman, J. V. Ortiz, J. Cioslowski, D. J. Fox, Gaussian Inc., Wallingford CT, **2009**.
[25] a) A. D. Becke, *J. Chem. Phys.* **1993**, *98*, 5648 – 5652; b) C. Lee, W. Yang, R. G. Parr, *Phys. Rev. B* **1988**, *37*, 785 – 789.
[26] a) A. D. McLean, G. S. Chandler, *J. Chem. Phys.* **1980**, *72*, 5639 – 5648; b) R. Krishnan, J. S. Binkley, R. Seeger, J. A. Pople, *J. Chem. Phys.* **1980**, *72*, 650 – 654; c) T. Clark, J. Chandrasekhar, G. W. Spitznagel, P. von R. Schleyer, *J. Comput. Chem.* **1983**, *4*, 294 – 301; d) M. J. Frisch, J. A. Pople, J. S. Binkley, *J. Chem. Phys.* **1984**, *80*, 3265 – 3269.

Received: July 8, 2014
Published online on October 21, 2014